Electronic structure, hyperfine interactions, and radial densities in the Fe^{1+} tetrahedral sulfide as calculated by the multiple-scattering method

S. K. Lie
Instituto de Física, Universidade Federal Fluminense, Caixa Postal 296, 24 210 Niterói, Rio de Janeiro, Brazil

M. Braga
Departamento de Química Fundamental, Universidade Federal de Pernambuco, 50 739 Recife, Pernambuco, Brazil

C. A. Taft
Centro Brasileiro de Pesquisas Físicas, rua Dr. Xavier Sigaud 150, 22 290 Rio de Janeiro, Rio de Janeiro, Brazil
(Received 30 December 1987; revised manuscript received 9 May 1988)

Spin-polarized multiple-scattering calculations have been performed for the FeS_4^{7-} cluster in order to investigate the uncommon Fe^{1+} charge state observed in ZnS. The calculated electronic structure, charge and spin densities, and atomic populations are used to interpret the measured hyperfine interactions. The overall good agreement between theory and experiment supports the presence of monovalent–charge-state Fe^{1+} in the Mössbauer spectra emitted by ^{57}Co diluted in ZnS.

I. INTRODUCTION

Most of the studies concerning the Mössbauer spectra of ^{57}Fe in iron sulfides[1–19] have been related to the Fe^{2+} and Fe^{3+} charge state. However, Garcin *et al.*[20] reported a ZnS:^{57}Co Mössbauer-source experiment in which a line attributed to Fe^{1+} was observed. The interpretation was based primarily on large isomer-shift values and deduced electronic configuration and the possible models for formation of Fe^{1+} were regarded as hypothetical in the absence of more direct evidence.

In our previous work the multiple-scattering method[21–23] with Slater's $X\alpha$ local exchange (MS-$X\alpha$) was applied to Fe(II), Fe(III), and Fe(IV) tetrahedral sulfide clusters in an effort to interpret various experimental results. We have thus considered it of interest to extend this work to the Fe(I) tetrahedral sulfide cluster in order to determine the electronic structure and Mössbauer hyperfine parameters of this interesting uncommon valence state and to investigate possible correlations with the experimental results.

II. METHOD OF CALCULATIONS

The MS-$X\alpha$ method[24] applied in this paper to the FeS_4^{7-} clusters is an *ab initio* one-particle approach in which the one-particle Schrödinger equations are solved numerically using a muffin-tin potential and Slater's $X\alpha$ local exchange. The values of atomic exchange parameters used in these calculations were taken from Schwarz: $\alpha(\mathrm{Fe})=0.711$, $\alpha(\mathrm{S})=0.724$, and $\alpha=0.721$ in the outersphere and intersphere region. The muffin-tin scheme employed assumed the Fe-sphere tangent to the sulfur spheres. We have used the Fe-S distance of 2.37 Å employed in our previous work in the Fe^{2+} (FeS_4^{6-}) cluster and the same Fe radius (2.21 a.u.) used for the three Fe^{2+}, Fe^{3+}, and Fe^{4+} iron sulfide clusters. Larsson's technique[25(a)] is used to derive atomic populations from the calculated MS-$X\alpha$ wave functions. The atomic populations are defined as

$$\rho_l = \sum_i n_i \frac{C_{il}^2}{K_l^2} , \tag{1}$$

where K_l is the amplitude of an atomic orbital used as reference orbital, C_{il} are the amplitude of the molecular orbitals, and n_i is the occupation of the orbital i. This is only an approximate way to define atomic charge, however, the results seem to be reasonably good and have been successfully applied to study charge transfer processes in transition-metal complexes containing π-acceptor ligands and hyperfine interactions in the Mössbauer and EPR spectroscopies.[21–23,25(b)]

III. ORBITALS, ORBITAL ENERGIES, HYPERFINE INTERACTIONS, RADIAL DENSITIES, AND ELECTRON POPULATIONS

The orbital energies obtained in a ground-state calculation in the spin-unrestricted formalism, the charge distribution within the muffin-tin region and the orbital characters labeled according to the irreducible representations of the symmetry group T_d for the FeS_4^{7-} cluster are given in Table I.

The $2t_1$ orbitals are mainly nonbonding ligand S $3p$ orbitals. The $6a_1$ and $6t_2$ are Fe $3s$ orbitals. The $7a_1$ and $7t_2$ are ligand $3s$ orbitals. The $8a_1$ orbitals are ligand $3p$ with some iron $4s$ component. The Fe $3d$–like crystal-field orbitals with small S $3p$ admixture are $3e\uparrow$, $10t_2\uparrow$, and $3e\downarrow$. The remaining orbitals $8t_2$, $2e$, and $9t_2$ are ligand S $3p$ orbitals with small Fe $3d$ admixture.

At the top of what would be termed the valence band is the filled $3e\downarrow$ orbital which is almost pure $3d$. The $8a_1$ orbitals are at the bottom of the valence band, whose width is 7.74 eV. Molecular orbitals below the valence

band show little or no mixing of Fe and S atomic orbitals.

In Table II we give the electron population for Fe in the FeS_4^{7-} cluster. The Fe $3d$ and $4s$ populations in the cluster are $3d\uparrow^{4.94}3d\downarrow^{1.90}4s\uparrow^{0.33}4s\downarrow^{0.28}$. The main difference between the actual configuration of iron in the FeS_4^{7-} and the Fe^{1+} ($3d^7$) free-ion configuration is the partial occupation of the $4s$ shells and a reduction of 0.16 electrons from $3d\uparrow$ and $3d\downarrow$ levels. The calculated net charge on the Fe atom is 0.59. The small decrease of 0.16 electrons in both $3d$ populations for the FeS_4^{7-} cluster

TABLE I. Orbital energies and orbital characters for FeS_4^{7-}. [Total charge: Fe sphere, 24.75; S sphere (each), 15.08; intersphere region, 10.94; outer sphere, 0.93.]

Orbital	Orbital energy ($-R_y$)	Charge[a] in muffin-tin sphere Fe	S[b]	Interatomic	Outer sphere	Orbital character
$1a_a\uparrow$	508.970	100				Fe $1s$
$1a_1\downarrow$	508.969	100				Fe $1s$
$2a_1\uparrow$	176.154		25			S $1s$
$2a_1\downarrow$	176.154		25			S $1s$
$1t_2\uparrow$	176.154		25			S $1s$
$1t_2\downarrow$	176.154		25			S $1s$
$3a_1\uparrow$	58.926	100				Fe $2s$
$3a_1\downarrow$	58.801	100				Fe $2s$
$2t_2\uparrow$	50.929	100				Fe $2p$
$2t_2\downarrow$	50.834	100				Fe $2p$
$4a_1\uparrow$	15.453		25			S $2s$
$4a_1\downarrow$	15.494		25			S $2s$
$3t_2\uparrow$	15.453		25			S $2s$
$3t_2\downarrow$	15.494		25			S $2s$
$5a_1\uparrow, 1e\uparrow, 1t_1\uparrow$ $4t_2\uparrow, 5t_2\uparrow$	11.593		25			S $2p$
$5a_1\downarrow, 1e\downarrow, 1t_1\downarrow$ $4t_2\downarrow, 5t_2\downarrow$	11.593		25			S $2p$
$6a_1\uparrow$	6.572	99.89	0.0	0.10	0.0	Fe $3s$
$6a_1\downarrow$	6.307	99.89	0.0	0.10	0.0	Fe $3s$
$6t_2\uparrow$	4.228	99.62	0.0	0.37	0.0	Fe $3p$
$6t_2\downarrow$	3.969	99.57	0.0	0.41	0.0	Fe $3p$
$7a_1\uparrow$	1.549	1.32	18.98	21.89	1.00	S $3s$
$7a_1\downarrow$	1.549	1.17	18.98	21.89	1.00	S $3s$
$7t_2\uparrow$	1.539	0.98	19.51	19.32	1.66	S $3s$
$7t_2\downarrow$	1.538	0.85	19.56	19.20	1.66	S $3s$
$8a_1\uparrow$	0.809	7.99	12.77	39.62	1.28	S $3p$,Fe $4s$
$8a_1\downarrow$	0.801	6.82	13.14	39.28	1.33	S $3p$,Fe $4s$
$8t_2\uparrow$	0.783	1.22	13.42	42.15	2.93	S $3p$,Fe $3d$
$8t_2\downarrow$	0.781	1.04	13.57	41.75	2.91	S $3p$,Fe $3d$
$2e\uparrow$	0.777	3.81	13.76	38.36	3.81	S $3p$,Fe $3d$
$2e\downarrow$	0.774	1.55	14.18	38.51	3.21	S $3p$,Fe $3d$
$9t_2\uparrow$	0.758	11.84	14.59	25.60	4.18	S $3p$,Fe $3d$
$9t_2\downarrow$	0.749	5.90	15.77	26.43	4.56	S $3p$,Fe $3d$
$2t_1\uparrow$	0.745	0.09	16.00	32.91	2.94	S $3p$
$2t_1\downarrow$	0.745	0.09	16.05	32.72	2.95	S $3p$
$3e\uparrow$	0.452	90.11	0.34	8.31	0.19	Fe $3d$,S $3p$
$10t_2\uparrow$	0.433	80.54	0.75	15.85	0.61	Fe $3d$,S $3p$
$3e\downarrow$[c]	0.240	81.11	0.43	15.88	1.27	Fe $3d$,S $3p$

[a]In % of one electron charge.
[b]In % of charge in each S sphere.
[c]Highest occupied level.

TABLE II. Electron population on Fe for molecular orbitals in the a_1, e, and t_2 symmetries for FeS_4^{7-}.

Symmetry	Atomic character	Spin up	Spin down
$6a_1$	$3s$	0.99	0.99
$7a_1$	$4s$	0.04	0.04
$8a_1$	$4s$	0.29	0.24
$2e$	$3d$	0.03	0.02
$3e$	$3d$	1.97	1.80
$6t_2$	$3p$	2.99	2.99
$7t_2$	$3d$	0.01	0.00
$8t_2$	$3d$	0.01	0.00
$9t_2$	$3d$	0.25	0.08
$10t_2$	$3d$	2.67	
Total	$3s$	0.99	0.99
charge	$3p$	2.99	2.99
	$3d$	4.94	1.90
	$4s$	0.33	0.28
Net charge on Fe (16 total)=0.59			

compared with the Fe^{1+} free ion is contrary to the trend observed in our previous calculations[21-23] of the FeS_4^{4-}, FeS_4^{5-}, and FeS_4^{6-} clusters (Table III). Those calculations indicated a substantial increase in the $3d$ population of 1.98, 1.05, and 0.22 electrons, respectively, relative to the free ion due to strong covalency in the Fe—S bond. There seems to be an opposite tendency in Fe^{+} (FeS_4^{7-}) clusters towards a reverse charge transfer process from the Fe^{1+} configuration thus defining the transient Fe^{+} charge state. We note from Table III that the calculated net Fe charge increases in the order of the increasing iron valency in the four sulfide clusters under discussion. We also see that the $3d$ and $4s$ populations for the different tetrahedral clusters show a regular pattern, i.e., $3d$ population increases from the FeS_4^{4-} to the FeS_4^{7-} cluster while the reverse is found for the $4s$ population. The same tendency is observed for the individual $3d$ and $4s$ spin-up and spin-down components. An exception is found for the FeS_4^{5-} cluster where the $3d\uparrow$ population is larger than the FeS_4^{6-} population and close to the corresponding free-ion value and the $3d\downarrow$ is smaller than the FeS_4^{4-} value. Experimental evidence[1] indicates that the $3d^5\uparrow$ configuration is preserved in the FeS_4^{5-} cluster. On the other hand, from Table I in Ref. 21 we notice that t_2 and e symmetries sum up to about 98.97% and 95.03%, respectively, of an electron inside the Fe sphere indicating that there is very little (if any) charge transfer for the completely occupied set of $3d$ spin-up orbitals. The same is also true for the sulfur ligands. Since some orbitals of $t_2\downarrow$ and $e\downarrow$ symmetries are unoccupied, the charge distribution in the lower-lying orbitals of the same symmetries and spin will give a very important contribution to the total $3d$ population. The basic correctness of our calculated $3d$ spin-up and spin-down occupancies is supported by the calculation of the magnetic susceptibilities and the number of unpaired $3d$ electron for the FeS_4^{5-} cluster[21] and the calculation of the quadrupole splitting for the FeS_4^{7-} cluster (see below). We note that the calculations indicate a Fe$\cong$1.2 effective electron charge in both the FeS_4^{4-} and FeS_4^{5-} clusters. The presence of a tetravelent iron in a sulfide is also not very likely, and it thus appears that the electron is back-donated to the iron thus reducing its charge. In going from Fe^{3+} to Fe^{2+}, i.e., from FeS_4^{5-} to FeS_4^{6-}, an electron is added to a mainly Fe orbital. On further reduction of Fe^{2+} to Fe^{1+}, i.e., from FeS_4^{6-} to FeS_4^{7-}, an additional electron may be added to a Fe orbital. However, the $3d$-type orbitals are partly buried in the sulfur $3p$ band and the additional electron may also be donated to an unoccupied energetically favorable S $3p$ orbital in order to regain the more stable Fe^{2+} charge state.

TABLE III. Net charge and $3d$ and $4s$ populations for FeS_4^{4-} FeS_4^{5-}, FeS_4^{6-}, and FeS_4^{7-} clusters.

Net Fe charge		$3d$ electron population	$4s$ electron population
$[Fe(IV)]S_4^{4-}$[a]	1.22	$3d\uparrow^{4.63}3d\downarrow^{1.35}$	$4s\uparrow^{0.44}4s\downarrow^{0.45}$
$[Fe(III)]S_4^{5-}$	1.20	$3d\uparrow^{4.94}3d\downarrow^{1.11}$	$4s\uparrow^{0.43}4s\downarrow^{0.42}$
$[Fe((II)]S_4^{6-}$[a]	1.07	$3d\uparrow^{4.83}3d\downarrow^{1.39}$	$4s\uparrow^{0.40}4s\downarrow^{0.41}$
$[Fe(I)]S_4^{7-}$	0.59	$3d\uparrow^{4.94}3d\downarrow^{1.90}$	$4s\uparrow^{0.33}4s\downarrow^{0.28}$

[a]Reference 23.
[b]Reference 21.

The Mössbauer isomer shift is defined as

$$\delta=\tfrac{2}{3}\pi Ze^2S(z)\Delta\langle r^2\rangle\{[\rho(0)]_A-[\rho(0)_S\}\ , \qquad (2)$$

where $\Delta\langle r^2\rangle$ is the change in the mean-square nuclear-charge radii in the Mössbauer transition (negative for Fe) and the term in brackets is the difference between the squared amplitude of the electronic wave function at the nucleus of absorber and source. $S(z)$ is a correction term for relativistic effects.

The iron sulfides show smaller values of isomer shifts due to the strong covalency of the Fe—S bonds. Isomer shifts for tetrahedral bonds are also smaller than for octahedral since the metal-ligand distances are shorter and both covalency and core distortions are correspondingly larger. The observed range for Fe^{3+} ions in tetrahedral sites of sulfur is only $0.18<\delta_{3+}(\text{tet})<0.20$ mm/s whereas the isomer shift for tetrahedral high-spin Fe^{2+} ions varies over a much larger range: $0.40<\delta_{2+}(\text{tet})<0.77$ mm/s.

In Table IV we give the total charge densities and individual contributions from different orbitals to the FeS_4^{7-} cluster. The values of the Fe^{1+} free ion are given for comparison. We note a small increase in the $2s$ and $3s$ densities on going from the free ion to the cluster. This may be ideally attributed to a small reduction of $3d$ electrons from a $3d^7$ configuration in the free ion to a $3d^{6.84}$ configuration in the cluster. The reduced screening will cause a contraction of mostly the $3s$ electron cloud because $r_{3s_{\max}}$ is even larger than $r_{3d_{\max}}$ which will result in an increase of the $3s$ contribution. In addition, we also observe a large $4s$ contribution for the FeS_4^{7-} cluster. The effect of the screening of $3s$ electrons together with

TABLE IV. Electron densities $|\psi(0)|^2$ ($|\psi(0)|^2 = \sum_i |\psi_\uparrow^i(0)|^2 + |\psi_\downarrow^i(0)|^2$) at the Fe nucleus for FeS_4^{7-} and Fe^{1+} free ion.

FeS_4^{7-}		Fe^{1+}	
$1a_1$ (Fe $1s$)	10 752.29	$1s$	10 752.71
$3a_1$ (Fe $2s$)	979.51	$2s$	979.16
$6a_1$ (Fe $3s$)	140.84	$3s$	140.14
$7a_1$	0.38		
$8a_1$	2.45		
Total	11 875.47		11 872.01

TABLE V. Spin densities χ ($\chi = 4\pi \sum_i | |u_\uparrow^i(0)|^2 - |u_\downarrow^i(0)|^2|$, where u^i is an occupied orbital of a_1 symmetry or an atomic s orbital) at the Fe nucleus and Fermi contact term H_c for FeS_4^{7-} and Fe^{1+} free ion.

FeS_4^{7-}		Fe^{1+}	
$1a_1$ (Fe $1s$)	−0.63	$1s$	−0.63
$3a_1$ (Fe $2s$)	−16.24	$2s$	−16.04
$6a_1$ (Fe $3s$)	7.56	$3s$	+6.90
$7a_1$	0.29		
$8a_1$	2.65		
Total	−6.37	Total	−9.77
$H_{cp}(kG)$	−268	H_c(KG)	−411

the $4s$ contribution are the major factors contributing to the difference in isomer shift of Fe^{1+}, Fe^{2+}, Fe^{3+}, and Fe^{4+} ions in the tetrahedral sulfur complexes.

From calculated charge densities (ρ_i, ρ_j) and measured isomer shifts (δ_i, δ_j) the isomer shift calibration constant is determined by

$$\delta_i - \delta_j = \alpha[\rho_i(0) - \rho_j(0)] , \tag{3}$$

where the lower index refers to different chemical compounds.

The experimental isomer shift[20] of the Fe^{1+} line in the ZnS matrix is large, i.e., 1.02±0.03 mm/s relative to $K_4Fe(CN)_6 3H_2O$ extrapolated to 300 K. In another experiment[26] the atoms produced by electron capture decay of ^{57}Co in Xenon matrix gives a Fe^{1+} state with atomic configuration $3d^7$ and a positive isomer shift (+1.77±0.08 mm/s) relative to iron metal at 300 K which we will approximate as our Fe^{1+} free-ion isomer-shift value. Using these experimental values, the electron densities for Fe^{1+} free ion and for FeS_4^{7-} cluster [Table IV and Eq. (3)] we obtain an isomer-shift calibration constant value of $\alpha = -0.22 a_0^3$ mm/s which is in very good agreement with the currently assumed value[27] of $-0.21 a_0^3$ mm/s.

Hoggins and Steinfink[18] have derived the equation $\delta = 1.4 - 0.4V$ which relates the isomer shift (δ) to the electrostatic valence V in iron tetrahedrally coordinated by sulfur compounds. Using this equation and the low-temperature isomer-shift value of the Fe^{1+} transient charge state in ZnS:^{57}Co Mössbauer source we obtain $V = 0.63$ which is in good agreement with our calculated net atomic charge of 0.59 (Table II).

In Fe^{1+}, the ground-state configuration is $3d^7, {}^4F$ ($L = 3, S = \frac{3}{2}$) which splits in cubic crystalline field into two orbitally degenerate triplets and one orbital singlet. The hyperfine field at the nucleus may be written as a sum of terms

$$H_{hf} = H_{cp} + H_{orb} + H_{dip} , \tag{4}$$

where H_{cp}, H_{orb}, and H_{dip} are the core polarization, orbital, and dipolar contributions.

The core polarization or Fermi contact term which is determined by the exchange polarization mechanism of the s shell by the unpaired d electrons is given by

$$H_{cp} = \tfrac{8}{3}\pi g \mu_B S[\,|\psi(0)|_\uparrow^2 - |\psi(0)|_\downarrow^2\,] , \tag{5}$$

where g is the electronic spectroscopic splitting factor, μ_B is the Bohr magneton, and S is the total spin. We obtain the spin densities at the nucleus from the a_1 orbitals having $l = 0$ in the iron sphere, determined from our spin-polarized calculations.

In Table V we give the total spin density at the Fe nucleus as well as the individual contributions from the different orbitals for the FeS_4^{7-} cluster. The Fe^{1+} free-ion values are given for comparison. We observe that the $1s$, $2s$, and $3s$ contributions are not substantially modified. This is contrary to our previous results in the Fe(II), Fe(III), and Fe(IV) sulfide clusters which indicated strong modifications of the $2s$ and $3s$ contributions due to the increased population of the $3d$ spin-down shell which via exchange polarization mechanism will reduce the negative and positive $2s$ and $3s$ spin contributions. In the present FeS_4^{7-} cluster, however, there have only been small changes in the $3d$ population and as a consequence the $2s$ and $3s$ contributions to the hyperfine field are not substantially modified. We note, however, as in the other sulfide clusters, a large positive contribution of 119 kG from $4s$ levels.

Since we have 3.04 unpaired d electrons, this work predicts hyperfines fields of ~88.16 kG per unpaired electron in the $3d$ shell. Since the Fe^{1+} free-ion hyperfine contact field is 1.53 times the Fe hyperfine contact field in the cluster we may make an order of magnitude estimate of 135 kG per unpaired electron for Fe^{1+} in more ionic compounds. Chappert *et al.*[28] obtained in the Mössbauer spectra of ^{57}Co-doped magnesium oxide a Fe^{1+} core polarization field of −127 kG per unpaired spin which is in good agreement with our order of magnitude estimate.

The observed quadrupole splitting due to the Fe^{1+} line in ZnS matrix is 1.80±0.05 mm/s, The valence shell contribution to the Mössbauer quadrupole splitting can be expressed as[29]

$$\begin{aligned} QS &= \tfrac{1}{2} e^2 q_{val} (1 - R) Q , \\ q_{val} &= \sum \langle (3\cos^2\theta - 1) \rangle \langle r^{-3} \rangle , \end{aligned} \tag{6}$$

R is the Sternheimer antishielding factor, Q is the quadrupole moment of the nucleus. By considering the symmetry of the wave functions the d-electron contribution to q_{val} can be expressed as

$$q_{\rm val}=K_d[-N_{d_{z^2}}+N_{d_{x^2-y^2}}+N_{d_{xy}}-\tfrac{1}{2}(N_{d_{xz}}+N_{d_{yz}})]\ , \quad (7)$$
$$K_d=\tfrac{4}{7}\langle r^{-3}\rangle_d\ .$$

We note from Eq. (7) that if the e and t_2 orbitals are all equally populated $q_{\rm val}=0$. If, however, there is some delocalization of metal electrons to ligands by charge donation a nonzero $q_{\rm val}$ can result and produce a quadrupole splitting.

It was thus considered of interest to investigate if our calculated $3d$ population can provide some rough estimate of the observed quadrupole splitting. We note that Finklea *et al.*[30] obtained in pyrite that

$$-N_{d_{z^2}}+N_{d_{x^2-y^2}}+N_{d_{xy}}-\tfrac{1}{2}(N_{d_{xz}}+N_{d_{yz}})=-0.0336$$

is the necessary $3d$ population change to produce a quadrupole splitting of 0.64 mm/s. In order to produce the observed quadrupole splitting of 1.80 mm/s attributed to the Fe^+ line a population unbalance of 0.0945 is required. We note from Table II that the difference between the average total e spin-up and spin-down $3d$ population is 0.09 which is in good agreement with our previously estimated value of 0.0945. This agreement should not be taken too seriously, however, considering the drastic approximations involved. The important conclusion is that our calculated $3d$ population can account for the order of magnitude of the observed quadrupole splitting.

From the experimental hyperfine parameters of the Fe^{1+} line in the ZnS matrix a $4s$ population of 0.60 has been deduced by Garcin *et al.*[20] In Table II we see that our calculations indicate a $4s$ population of 0.61 in agreement with the experimental results.

We give in Figs. 1–3 the Fe $3d$ (e and t_2 orbitals) as well as Fe $4s$ (a_1 orbitals) radial densities. The Fe^{1+} HF-$X\alpha$ ($\alpha=0.71$) $3d$ and $4s$ radial densities are also given for comparison. The $3e\uparrow$, $3e\downarrow$, and $10t_2\uparrow$ are Fe $3d$-type orbitals with a very small S $3p$ admixture whose radial functions have nearly an atomiclike $3d$ shape, with maximum in the same region, and are not delocated with respect to the maximum of the atomic $3d$ function. The $8t_2$, $9t_2$, and $2e$ orbitals are ligand S $3p$ with small Fe $3d$ admixture. As opposed to our previous work in Fe^{2+}, Fe^{3+}, and Fe^{4+} tetrahedral clusters, there is much less admixture between the Fe $3d$ and S $3p$ orbitals.

The $4s$ valence shell has a smaller charge density at nucleus than the core s shells, however, being closest to the valence $3d$ electrons it feels changes in ionicity, i.e., in number of $3d$ electrons, more strongly and produces the largest changes between free-ion and the cluster electron

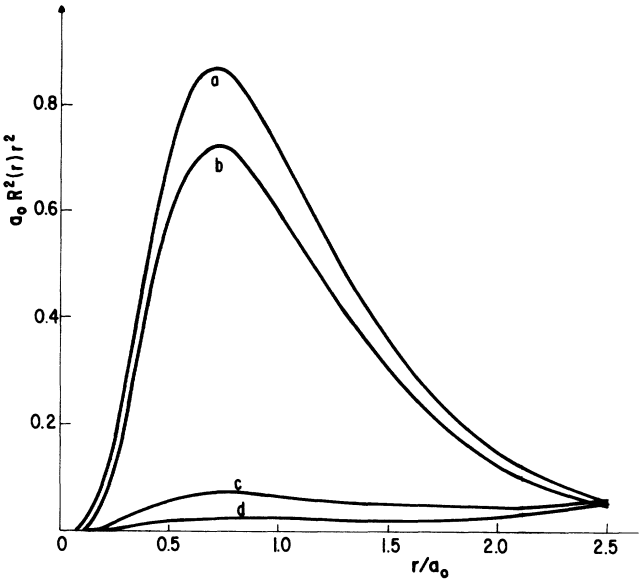

FIG. 2. Radial densities of orbitals (a) Fe^{1+} $3d$ HF $X\alpha$; (b) $10t_2\uparrow$; (c) $9t_2\uparrow$; (d) $9t_2\downarrow$.

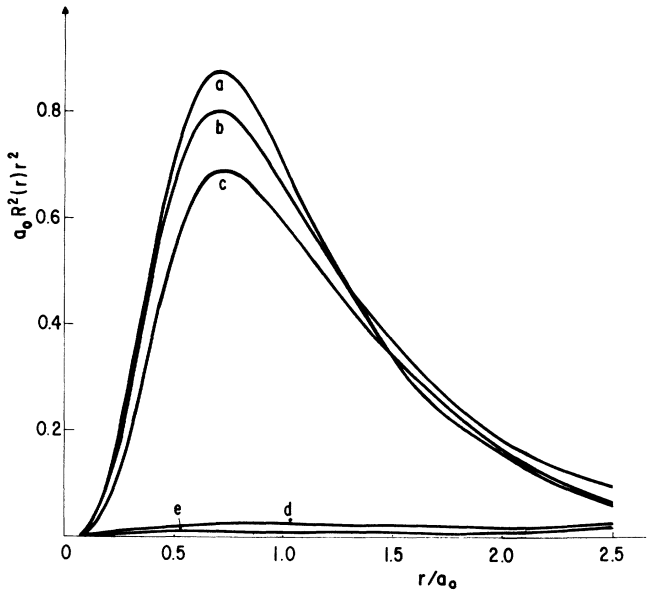

FIG. 1. Radial densities of orbitals (a) Fe^{1+} $3d$ HF $X\alpha$; (b) $3e\uparrow$; (c) $3e\downarrow$; (d) $2e\uparrow$; (e) $2e\downarrow$.

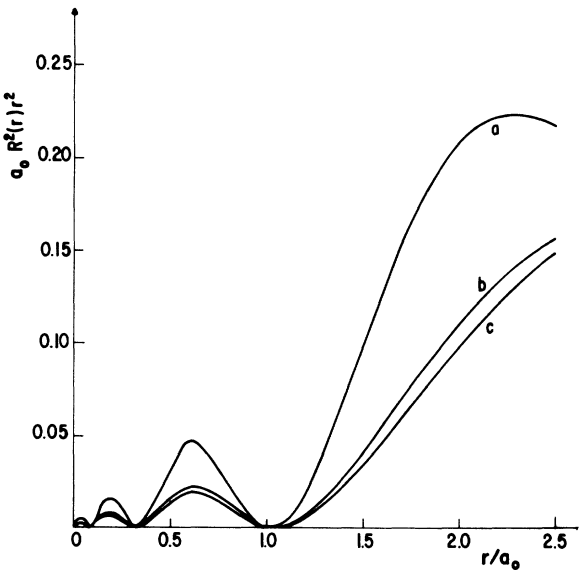

FIG. 3. Radial densities of orbitals (a) Fe HF $X\alpha$ $4s$ (scale $\frac{1}{2}$); (b) Fe $4s\uparrow$ ($8a_1\uparrow$); (c) Fe $4s\downarrow$ ($8a_1\downarrow$).

densities at Fe nucleus. In the iron sulfide clusters the $4s\uparrow$ density is larger than the $4s\downarrow$ density and together they sum a large contribution to isomer-shift effects, and result in a substantial positive contribution to the Fermi contact term (H_c) causing a large covalent reduction of the negative hyperfine field.

The overall good agreement between the theory and experiment leads us to conclude that our calculated electronic structure, hyperfine parameters, electron population, and radial densities correlate well with the hyperfine parameters obtained from the experimental Mössbauer investigation and thus support the assignment of an uncommon Fe^{1+} charge state in ZnS.

[1]C. A. Taft, D. Raj, and J. Danon, International Conference Proceedings on Mössbauer Spectroscopy, Bendor, France (1974) (unpublished); J. Phys. (Paris) Colloq. **35**, C6-241 (1974); J. Phys. Chem. Solids **36**, 283 (1975).

[2]C. A. Taft, S. F. Cunha, N. G. Souza, and N. C. Furtado, J. Phys. Chem. Solids **41**, 61 (1980).

[3]C. A. Taft, J. Phys. (Paris) **38**, 15 (1977).

[4]R. B. Scorzelli, C. A. Taft, J. Danon, and V. K. Garg, J. Phys. C **11**, 1397 (1978).

[5]R. S. de Biasi, C. A. Taft, and N. C. Furtado, J. Magn. Magn. Mater. **23**, 211 (1981).

[6]T. P. Arsenio, Z. Arguello, P. H. Domingues, N. C. Furtado, and C. A. Taft, Phys. Status Solidi **110**, K129 (1982).

[7]C. A. Taft and M. A. de Paoli, Chem. Phys. Lett. **68**, 94 (1979).

[8]P. H. Domingues, T. P. Arsenio, N. C. Furtado, and C. A. Taft, Phys. Status Solidi B **14**, K161 (1982).

[9]D. M. Cooper, D. P. E. Dickson, P. H. Domingues, G. P. Gupta, C. E. Johnson, M. F. Thomas, C. A. Taft, and P. J. Walker, J. Magn. Magn. Mater. **36**, 171 (1983).

[10]R. S. de Biasi, C. A. Taft, and N. C. Furtado, J. Magn. Magn. Mater. **21**, 125 (1980).

[11]T. P. Arsenio, P. H. Domingues, and C. A. Taft, Phys. Status Solidi B **105**, K31 (1981).

[12]D. J. Vaughan and J. R. Craig, *Mineral Chemistry of Metal Sulfides* (Cambridge University Press, New York, 1978).

[13]P. H. Domingues, J. M. Neto, C. A. Taft, N. C. Furtado, and T. P. Arsenio, Solid State Commun. **56**, 193 (1985).

[14]R. S. de Biasi, C. A. Taft, and N. C. Furtado, J. Mater. Sci. Lett. **5**, 1191 (1986).

[15]I. L. Torriani, Z. P. Arguello, A. R. Freiria Filho, J. P. Suassuna, and C. A. Taft, J. Mater. Sci. **23**, 1068 (1986).

[16]R. S. de Biasi, C. A. Taft, and N. C. Furtado, J. Mater. Sci. Lett. **6**, 1185 (1987).

[17]Y. K. Sharma, L. Iannarella, F. E. Wagner, C. A. Taft, N. C. Furtado, and T. P. Arsenio, Hyperfine Interact **41**, 517 (1988).

[18]J. T. Hoggins and H. Steinfink, Inorg. Chem. **15**, 1682 (1976).

[19]M. Eibschutz, S. Shtrikman, and Y. Tenenbaum, Phys. Lett. **24A**, 563 (1967); M. R. Spender and A. H. Morrish, Can. J. Phys. **50**, 1125 (1972).

[20]C. Garcin, P. Imbert, G. Jéhanno, A. Gérard, and J. Danon, J. Phys. Chem. Solids, **41**, 969 (1980).

[21]C. A. Taft and M. Braga, Phys. Rev. B **21**, 5802 (1980).

[22]S. K. Lie and C. A. Taft, Chem. Phys. Lett. **89**, 463 (1982).

[23]S. K. Lie and C. A. Taft, Phys. Rev. B **28**, 7308 (1983).

[24]K. H. Johnson, J. Chem. Phys. **45**, 3085 (1966); Adv. Quantum Chem. **7**, 143 (1973); J. C. Slater and K. H. Johnson, Phys. Rev. B **5**, 844 (1972).

[25](a) S. Larsson, Theor. Chem. Acta **49**, 45 (1978); (b) S. Larsson and M. Braga, Int. J. Quantum Chem. **15**, 1 (1979); M. Braga, S. Larsson, and J. R. Leite, J. Am. Chem. Soc. **101**, 3867 (1979); M. Braga, A. C. Pavão, and J. R. Leite, Phys. Rev. B **23**, 4328 (1981).

[26]H. Miklitz and P. H. Barrett, Phys. Rev. Lett. **28**, 1547 (1972).

[27]J. Danon, *IAEA Panel on the Applications of the Mössbauer Effect in Chemistry and Solid State Physics* (International Atomic Energy Agency, Vienna, 1966), p. 89.

[28]J. Chappert, R. B. Frankel, A. Misetich, and N. A. Blum, Phys. Rev. **179**, 578 (1969).

[29]G. M. Bancroft, *Mössbauer Spectroscopy. An Introduction for Chemists and Geochemists* (Wiley, New York, 1973).

[30]S. L. Finklea III, LeConte Calhey, and E. L. Alma, Acta Crystallogr. A **32**, 529 (1976).